arXiv:1505.01023v1 [cond-mat.stat-mech] 5 May 2015

Fractal Liquids

Marco Heinen,[1,*] Simon K. Schnyder,[2] John F. Brady,[1] and Hartmut Löwen[3]

[1]Division of Chemistry and Chemical Engineering, California Institute of Technology, Pasadena, California 91125, USA
[2]Department of Chemical Engineering, Kyoto University, Kyoto 615-8510, Japan
[3]Institut für Theoretische Physik II, Weiche Materie,
Heinrich-Heine-Universität Düsseldorf, 40225 Düsseldorf, Germany

(Dated: May 6, 2015)

We introduce fractal liquids by generalizing classical liquids of integer dimensions $d = 1, 2, 3$ to a fractal dimension d_f. The particles composing the liquid are fractal objects and their configuration space is also fractal, with the same non-integer dimension. Realizations of our generic model system include microphase separated binary liquids in porous media, and highly branched liquid droplets confined to a fractal polymer backbone in a gel. Here we study the thermodynamics and pair correlations of fractal liquids by computer simulation and semi-analytical statistical mechanics. Our results are based on a model where fractal hard spheres move on a near-critical percolating lattice cluster. The predictions of the fractal Percus-Yevick liquid integral equation compare well with our simulation results.

PACS numbers: 61.20.Gy 61.20.Ja 61.43.Hv

The liquid state, as intermediate between gas and solid, is characterized by significant particle pair correlations indicating short-ranged, isotropic order around a tagged particle in surrounding shells [1]. While the shell structure is lost for a gas, the solid exhibits long-ranged correlations and anisotropy. Particle pair correlations are accessible by experiments [2, 3] and contain valuable information about the particle interactions. The latter are typically described by a pairwise additive interaction potential such as, e.g., hard spheres or Lennard-Jones. A fundamental task in theory and computer simulation of the liquid state is to predict the pair correlations for a given interaction. In this respect, one particularly successful approach is liquid integral equation theory [1, 4].

Molecular and colloidal liquids can be restricted to one or two spatial dimensions [5, 6] by confining them on substrates [7], at interfaces [8], between plates [9, 10] or in channeled matrices [11] or optical landscapes [12]. The thermodynamic properties change accordingly [13] and the system is called a one-dimensional or two-dimensional liquid. While all these classical examples of ideally confined liquids involve an integer-dimensional configuration space, there are also realizations and models where liquids are confined in a porous medium [14–17], or moving along a quenched polymer coil [18]. In the latter two cases, the configuration space along which the particles move is characterized by a non-integer (fractal) dimension d_f at suitable length scales. Much work has been devoted to understanding the two extreme cases of low and high density, namely the motion of single particles on a fractal (see, e.g., [19–23]) and the structure factor of a fractal aggregate itself, which can be considered as a particulate system at very high density where all particles are arrested [24–28]. In all of these situations, the interaction between the particles occurs in the embedding integer-dimensional space and the interaction energy depends on the Euclidean distance between particles.

In this letter, we break new grounds by considering fractal particles in a fractal configuration space, both of the same non integer dimension d_f. The interaction between two of these fractal particles is not described by a pair potential in Euclidean space, but instead inherits fractal elements both from the underlying configuration space and the fractal nature of the particles. Unifying the two complementary fields of classical liquid state theory and fractal structures, we refer to the explored, dense disordered phases as 'fractal liquids'. Our approach is 'microscopic' in the sense that it is particle-resolved, as opposed to continuum mechanical descriptions of fluid flow on fractals [29, 30].

Not only are fractal liquids interesting from a purely theoretical perspective of statistical mechanics, but realizations of such liquids can occur in nature. Microporous media filled with a phase-separating binary fluid such as a water and oil mixture are found in natural oil or gas reservoirs, and are produced during hydraulic fracturing in oil drilling. If the size of the oil droplets largely exceeds the porosity length scale, they adapt to the fractal shape of the void space. Such droplets constitute fractal 'particles' that are interacting in a fractal configuration space set by the voids of the porous medium. This realization of our model can be readily generalized to include other kinds of 'particles', such as floppy slime molds [31] or fluid droplets confined to other fractal aggregates like, e.g., the polymers constituting a macroscopic gel.

Here we develop the basic concepts for the statistical mechanics of fractal liquids. We present Monte Carlo simulations along with a semi-analytical fractal liquid integral equation approach. The liquid integral equation is shown to predict the particle pair-correlation functions and the thermodynamics of fractal liquids at high accuracy, qualifying the method as a powerful tool for studying fractal liquids. We exemplify this for a fractal hard sphere liquid, the analogue of the generic standard model

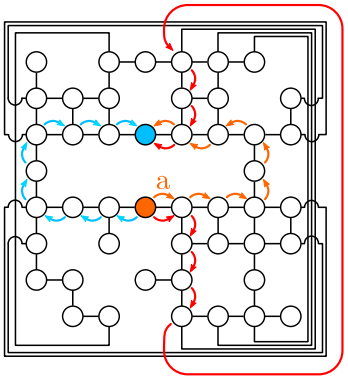

Fig. 1: Lattice schematic. From an 8×8 square lattice with periodic boundaries, 17 vertices have been removed. The remaining 47 vertices are depicted as circles. The black lines are the bonds of length a between the vertices. The chemical distance between the orange and the blue filled circle is $r_c = 8a$ along any of the three paths indicated by red, blue and orange arrows. The Euclidean distance between the orange and the blue filled circles is $2a$. All lattices used in our simulations have millions of vertices.

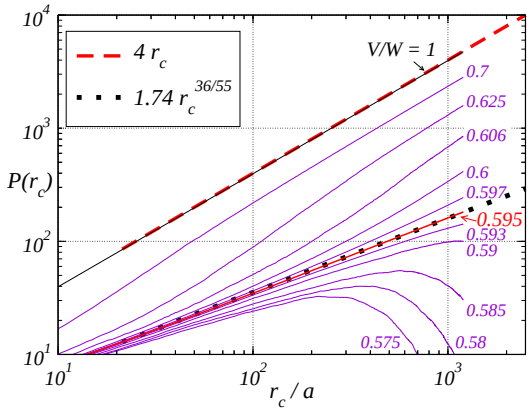

Fig. 2: Fractal cluster size scaling. The solid curves indicate the average numbers, $P(r_c)$, of vertices with chemical distance r_c from a tagged vertex, in the largest cluster remaining from a square lattice of initially $W = 3000 \times 3000$ vertices. Results are for various numbers $W - V$ of removed vertices, with ratios V/W as indicated. The number of vertices in the largest cluster is in general less than V. Results for the near-critical ratios $V/W = 0.593$, 0.595 and 0.597 are each averaged over 200 independent grid realizations. Upper dashed line: $P(r_c) = 4\, r_c$, corresponding to a two-dimensional lattice. Lower dotted line: $P(r_c) = 1.74\, r_c^{36/55}$, corresponding to a 91/55-dimensional lattice. The lattices used in our simulations are for $V/W = 0.595$.

of liquids in integer dimensions.

In order to model a fractal liquid we first need to construct a fractal dimensional space with a well-defined measure of distance, in which the particles can move. A viable choice of such space is a large set of vertices to serve as a discrete lattice in a fractal lattice liquid simulation. Starting from a regular square lattice with a total number W of vertices and with periodic boundary conditions in an embedding two-dimensional Euclidean space, we remove vertices at random until a number V of vertices is left. According to the results of percolation theory [20, 32], in the limit of $W \to \infty$ there is a critical site percolation threshold $p_c = V/W$ at which a percolating cluster with fractal spatial dimension is observed that extends to infinite length scales. For the square lattice, a threshold of $p_c = 0.5927\ldots$ has been reported [33].

In what follows, all distances r_c between vertices are evaluated as shortest distances on the graph that parametrizes the percolating cluster, using our own implementation of what is in essence equal to Dijkstra's algorithm [34]. The distance between any two vertices is $r_c = a$ iff the two vertices are connected by a bond in one of the two Cartesian directions in which the grid boundaries are connected periodically. Diagonal bonds are not implemented (i.e. a diagonal vertex pair has a minimum distance of $r_c = 2a$). Illustrated in Fig. 1, this measure of distance is commonly referred to as the 'chemical distance' and the corresponding non Euclidean metric is known as the 'taxicab metric' or 'Manhattan metric'.

The parameters of the lattice in Fig. 1 are $W = 64$ and $V = 47$. This small lattice features the essential properties of the lattices in our simulations, except of their much larger size of $W = 3000 \times 3000$, $V = 5\,355\,000$.

The ratio $V/W \approx 0.595$ for the simulations is 0.4% above the percolation threshold p_c for infinite lattices. This slight subcriticality is chosen to ensure the presence of a fractal percolating cluster in the finite system, as shown in Fig. 2: The average number $P(r_c)$ of vertices with chemical distance r_c from a tagged vertex obeys a non-integer exponent power law $P(r_c) \propto r_c^{36/55}$.

The chemical distance fractal dimension of the percolating square lattice cluster has been calculated exactly [20, 35] and was found to be $d_f = 91/55 \approx 1.655$. This is in agreement with our measurement, where $P(r_c) \propto r_c^{(d_f-1)}$. Note that the value $d_f = 91/55$ differs from the more commonly reported fractal dimension 91/48 of the cluster, which is found when distances are measured in the Euclidean metric [20, 32].

In our simulations we only use those vertices that belong to the largest, percolating cluster. All other vertices, either belonging to smaller clusters or being isolated, are deleted before a simulation is started. An average number of around 3×10^6 vertices remain, all of which are connected.

We define a fractal particle as the set of vertices that belong to the percolating cluster, and that are within a distance $r_c \le \sigma/2$ from a center vertex (and σ is an even number in our simulations). Every particle has exactly one center vertex and we refer to σ as the particle diameter. The Monte Carlo moves (described below) are implemented in a way that guarantees every particle to occupy at least one pair of vertices (v_1, v_2) with a chemical dis-

tance of σ at all times. Particles interact by a no overlap constraint which prohibits configurations in which any two particle center vertices have a distance of $r_c \leq \sigma$. All our simulations are for $\sigma = 300a$, a length scale at which the percolating cluster clearly exhibits fractal dimension (c.f. Fig. 2). Thus, the particles themselves are fractal objects. As the simulation snapshot in Fig. 3 shows, the particles are anisotropic in the two-dimensional embedding space, and a particle center vertex is not necessarily located anywhere near the particle's center of mass in the embedding space. However, in the fractal-dimensional space of the percolating cluster and in taxicab metric, each particle is a perfectly isotropic object, and the no-overlap interaction is also isotropic. In spite of their dramatically different appearance in embedding space, all particles are indistinguishable for all purposes of our simulation. Therefore, the simulated particles can be interpreted as an analogue of monodisperse hard spheres in fractal dimension, and one may refer to the simulated system as the 91/55-dimensional hard sphere liquid.

We simulate the thermodynamic equilibrium state of fractal particle ensembles on the fractal cluster, according to the classical rules of Monte Carlo simulation. Particles are moved one at a time, and every move is implemented as follows:

First, a particle is picked at random and removed from the system. Then we pick a random vertex v_1 globally from the cluster. Vertex v_1 is a candidate to become a vertex at the rim of the displaced particle. We compute the set M of all vertices with a distance $r_c = \sigma$ from vertex v_1, and we pick randomly a vertex v_2 out of M. Vertex v_2 is a second candidate to be at the rim of the displaced particle, together with vertex v_1. We compute the set K of vertices with distance $\sigma/2$ to both vertices v_1 and v_2. From the set K we randomly pick a vertex v_3, which is the candidate to become the center vertex of the displaced particle. If there is a center vertex of another particle within chemical distance $r_c \leq \sigma$ from vertex v_3, then the move is rejected and the original particle is restored. Otherwise, the move is accepted.

The simulation starts with a random configuration of potentially overlapping particles with a small diameter of $\sigma = 10a$. At early stages of the simulation, σ is gradually increased at a slow rate until the target value $\sigma = 300a$ is reached. This initial inflation facilitates finding a dense configuration without overlaps. After the initial inflation and equilibration stage the production stage is entered. During production stage, we record the average number $N(r_c)$ of particles with center-to-center chemical distance r_c. Binning of the function $N(r_c)$ with a bin width of $r_c = 5a$ is implemented in order to reduce scatter in the data. Inside a fractal control volume, the fractal packing fraction ϕ is measured as the average ratio of the number of vertices occupied by particles, divided by the total number of vertices in the control volume. The control volume is a set of vertices belonging to the cluster, each of which has a chemical distance of $r_c \leq 1500a$ from a center vertex. It is randomly moved throughout the simulation and contains at least one vertex pair with distance $r_c = 3000a$ at all times.

As expected, the recorded function $N(r_c)$ scales proportional to $r_c^{d_f-1}$ at large values of r_c. We compute the chemical distance distribution function $g(r_c)$ as

$$g(r_c) = c \ \times \ N(r_c) \ / \ r_c^{36/55}, \tag{1}$$

with the r_c-independent constant c chosen such that $g(r_c) \to 1$ for large r_c. The chemical distance distribution function is the analogue of the radial distribution function $g(r)$ of isotropic liquids in integer dimensions [1].

Since all distances are computed by Dijkstra's algorithm our simulations require long runtimes. The ramified structure of the percolating cluster prevents an efficient implementation of lookup tables or divide-and-conquer approaches for distance calculation. The only obvious way to improve the numerical performance of the Monte Carlo algorithm is parallel execution of statistically independent runs and subsequent averaging, as done in our simulations.

The Ornstein-Zernike integral equation for a homogeneous and isotropic liquid in Euclidean space with an integer dimension d reads

$$g(r) = 1 + c(r) + n \int d^d\boldsymbol{r}'[g(r') - 1] \ c(|\boldsymbol{r} - \boldsymbol{r}'|), \tag{2}$$

where n is the d-dimensional particle number density, $c(r)$ is the direct correlation function [1], $\boldsymbol{r}$ is a d-dimensional vector with Euclidean norm $r = |\boldsymbol{r}|$, and $d^d\boldsymbol{r}'$ is an infinitesimal d-dimensional volume element at position $\boldsymbol{r}'$. In conjunction with the no overlap constraint $g(r \leq \sigma) = 0$ and the approximation $c(r > \sigma) = 0$, Eq. (2) constitutes the Percus-Yevick integral equation for d-dimensional hard spheres, which can be systematically derived by functional Taylor expansion [1].

We solve the Percus-Yevick equation by means of a spectral solver [37]. Our numerically efficient algorithm for the convolution-type Eq. (2) is based on the Fourier-Bessel (Hankel) transform pair

$$\tilde{f}(q) \ = \ \frac{(2\pi)^{d/2}}{q^{d/2-1}} \int_0^\infty dr \ r^{d/2} f(r) J_{d/2-1}(qr), \tag{3}$$

$$f(r) \ = \ \frac{r^{1-d/2}}{(2\pi)^{d/2}} \int_0^\infty dq \ q^{d/2} \tilde{f}(q) J_{d/2-1}(qr), \tag{4}$$

for an isotropic function f in d dimensions, sampled on computational grids with exponentially increasing spacing between gridpoints [38–40]. In Eqs. (3) and (4), $J_{d/2-1}(x)$ denotes the Bessel function of the first kind and order $d/2 - 1$. Since $J_{d/2-1}(x)$ is analytic with respect to both x and d, the solution can be carried out

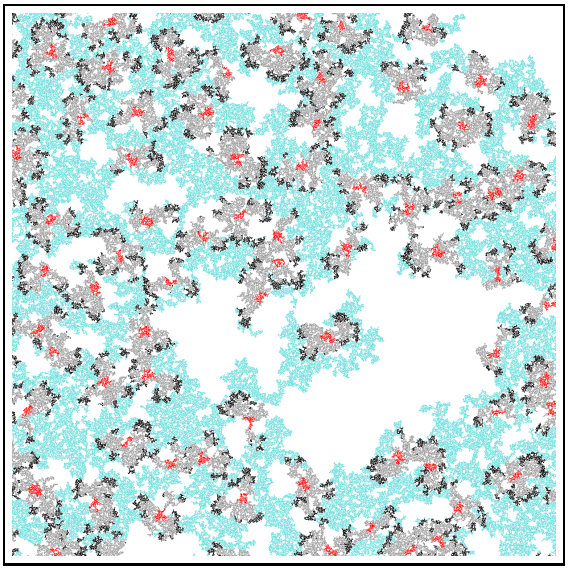

Fig. 3: Snapshot of a Monte Carlo simulation in the equilibrated state. Three hundred particles of diameter $\sigma = 300a$ are simulated on the largest (percolating) cluster that remains after 3 645 000 random vertices have been removed from a $3000a \times 3000a$ square lattice. The white spaces are inaccessible for the particles. Light blue: Fractal cluster on which the particles are allowed to move. Gray, red and black: Vertices occupied by particles. Red: Particle center regions (chemical distance to a particle center is less than 0.1σ). Black: Particle rim regions (chemical distance to a particle center is more than 0.4σ and less than 0.5σ). Gray: Regions where the chemical distance to a particle center is more than 0.1σ and less than 0.4σ. Every pixel in the figure corresponds to one vertex in the simulation. Only one quarter of the simulation box is shown, containing here 72 particle centers.

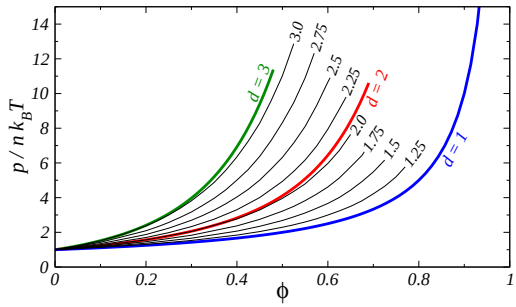

Fig. 4: Equations of state for hard spheres in dimensions from $d = 1$ to $d = 3$. Thick blue curve: Exact (Tonks gas / PY) result for $d = 1$. Thick red curve: Kolafa-Rottner [36] virial series with 15 coefficients for $d = 2$. Thick green curve: Carnahan-Starling equation of state for $d = 3$. Thin black curves are the PY virial pressure results for dimensions as indicated.

formally also for non integer values of d. The resulting pair-correlations and thermodynamic properties represent the analytic continuations of the standard (integer dimension) Percus-Yevick theory to non integer dimensions.

Thermodynamic properties of liquids in arbitrary dimensions can be efficiently calculated by means of a suitable liquid integral equation. This is demonstrated in Fig. 4 which features equations of state for hard spheres in various dimensions from $d = 1$ to $d = 3$. Thin black curves in Fig. 4 represent the d-dimensional hard sphere reduced virial pressure

$$\frac{p}{nk_BT} = 1 + 2^{(d-1)}\phi g(r = \sigma^+) \qquad (5)$$

with Boltzmann constant k_B, absolute temperature T, d-dimensional packing fraction $\phi = 2\pi^{d/2}(\sigma/2)^d n/d\Gamma(d/2)$ in terms of the Gamma function, and $g(r)$ calculated in the PY scheme. In Eq. (5), $g(r = \sigma^+)$ is the contact value of the radial distribution function, analytically continued with respect to the dimension. Exact or nearly exact reference solutions for $d = 1, 2$ and 3 are shown as thick curves in Fig. 4. For $d = 1$, the PY result reduces to the exact (Tonks gas) solution $p/nk_BT = 1/(1-\phi)$. Note the good agreement of the PY-scheme result with the numerically accurate virial series from Ref. [36] for $d = 2$, verifying the good accuracy of the PY scheme for dimensions in the range from $d = 1$ to $d = 2$. Increasing inaccuracy of the PY scheme for higher dimensions and large packing fractions is revealed in comparison to the nearly exact Carnahan-Starling equation of state $p/nk_BT = (1 + \phi + \phi^2 - \phi^3)/(1-\phi)^3$ for $d = 3$.

Figure 5 shows the chemical distance distribution functions $g(r_c)$ extracted from our simulations for systems of 300 and 150 particles. Also shown are the functions $g(r)$ that are the solutions of the PY integral equation for dimensions $d = 1$, $d = d_f = 91/55$ and $d = 2$ and for (fractal) packing fractions $\phi = 0.487$ and 0.266, as indicated in the figure legends. With the values of ϕ determined in the simulation as described above, the PY integral equation scheme is free of adjustable parameters. The solutions of the PY equation for $d_f = 91/55$ (thick red curves) agree best with the simulation data. This is most clearly revealed in the upper panel of Fig. 5, for the higher density liquid.

In conclusion, we have shown how to simulate dense disordered liquid phases of fractal particles in thermodynamic equilibrium and in fractal configuration space, and we have demonstrated that the particle correlations in such fractal liquids can be semi-analytically calculated by solving a liquid integral equation. The results shown here could be straightforwardly extended to other fractal dimensions. For example, a fractal liquid on a percolating simple cubic lattice embedded in three dimensional Euclidean space should exhibit a dimension between 2 and 3. Particle interactions different from the simple no overlap (fractal hard sphere) interactions should be studied in future, including short ranged attractive interactions that can be expected to lead to liquid-vapor demixing, and long-ranged repulsive interactions including the ultimately long-ranged Coulomb interaction. The generic

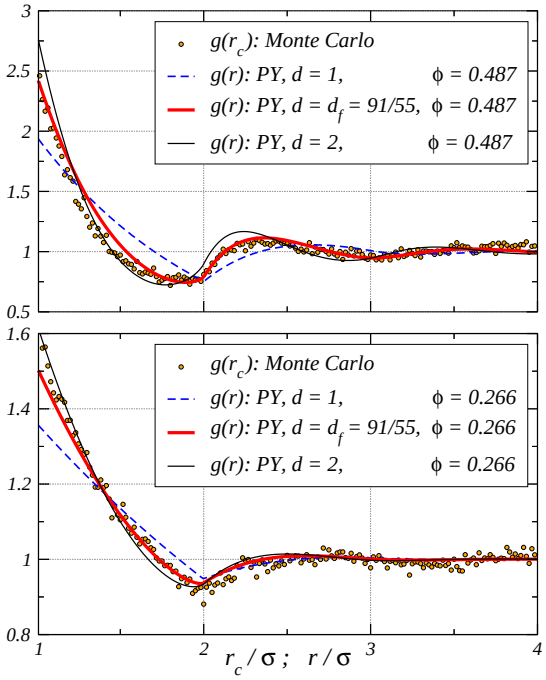

Fig. 5: Symbols: Chemical distance distribution functions $g(r_c)$ from our Monte Carlo simulations. Solid lines: PY solutions for $g(r)$, for dimensions and (fractal) packing fractions as indicated. The top panel is for a simulation of 300 particles, and the lower panel is for 150 particles. All other parameters are the same as for Fig. 3.

model system that we have presented here consists of monodisperse fractal particles, but polydispersity in the particle interactions is already implemented in the liquid integral equation solver which is going to facilitate future research on polydisperse fractal liquids.

Studying fractal liquids paves the way to a plethora of new fundamental research. One topic that naturally comes to mind concerns phase transitions in non integer dimensions. At present it is unclear which types of thermodynamic phases exist in fractal dimension and we do not know whether symmetry breaking and crystallization can occur in such spaces. Field theories like density functional theory could be extended into fractal dimension, in a similar way as we have demonstrated it for the PY integral equation. Mode coupling theory of the kinetic glass transition, which has been discussed for three-dimensional liquids in porous media [41] and in arbitrary dimensions [42, 43] relies on static structure as an input, which can be calculated using fractal liquid integral equations. While we have restricted ourselves here to studying the thermodynamic equilibrium state of a fractal liquid, future studies should include time-resolved dynamics of fractal liquids in and out of equilibrium. Transport coefficients of fractal liquids may be studied, requiring a precise account of hydrodynamic interactions in fractal geometry. A promising application for the theory of fractal liquids is the prediction of thermodynamic properties of microphase separated two-phase flow in porous media as encountered, for example, in oil and gas reservoirs and in oil production by hydraulic fracturing.

We thank Matilde Marcolli, Jürgen Horbach, Stefan U. Egelhaaf, Charles G. Slominski, Ahmad K. Omar and Mu Wang for numerous discussions that helped to develop the ideas presented here. This work was supported by the ERC Advanced Grant INTERCOCOS (Grant No. 267499) and by the graduate school POROSYS. M.H. acknowledges support by a fellowship within the Postdoc-Program of the German Academic Exchange Service (DAAD).

* mheinen@caltech.edu

[1] J.-P. Hansen and I. R. McDonald. Theory of Simple Liquids. Elsevier Academic Press, Amsterdam, 3rd edition, 2006.
[2] W.K. Kegel and A. van Blaaderen. Science, 287:290–293, 2000.
[3] C. P. Royall, S. R. Williams, T. Ohtsuka, and H. Tanaka. Nature Materials, 7:556–561, 2008.
[4] C. Caccamo. Phys. Rep., 274:1–105, 1996.
[5] C. Alba-Simionesco, B. Coasne, G. Dosseh, G. Dudziak, K. E. Gubbins, R. Radhakrishnan, and M. Sliwinska-Bartkowiak. J. Phys.-Condes. Matter, 18:R15–R68, 2006.
[6] M. Schoen and S. Klapp. Nanoconfined fluids: Soft matter between two and three dimensions. Reviews in computational chemistry, 24:1–509, 2007.
[7] S. Deutschländer, T. Horn, H. Löwen, G. Maret, and P. Keim. Phys. Rev. Lett., 111:098301, 2013.
[8] K. Zahn and G. Maret. Phys. Rev. Lett., 85:3656–3659, 2000.
[9] S. Neser, C. Bechinger, P. Leiderer, and T. Palberg. Phys. Rev. Lett., 79:2348–2351, 1997.
[10] M. C. Stewart and R. Evans. J. Chem. Phys., 140:134704, 2014.
[11] K. Hahn, J. Kärger, and V. Kukla. Phys. Rev. Lett., 76:2762–2765, 1996.
[12] Q.-H. Wei, C. Bechinger, and P. Leiderer. Science, 287:625–627, 2000.
[13] T. Franosch, S. Lang, and R. Schilling. Phys. Rev. Lett., 109:240601, 2012.
[14] J. Kurzidim, D. Coslovich, and G. Kahl. Phys. Rev. Lett., 103:138303, 2009.
[15] K. Kim, K. Miyazaki, and S. Saito. J. Phys. Condens. Matter, 23:234123, 2011.
[16] T. O. E. Skinner, S. K. Schnyder, D. G. A. L. Aarts, J. Horbach, and R. P. A. Dullens. Phys. Rev. Lett., 111:128301, 2013.
[17] S. Torquato. Random heterogeneous materials: microstructure and macroscopic properties, volume 16. Springer Science & Business Media, 2002.
[18] J.-L. Barrat and J.-P. Hansen. Basic Concepts for Simple and Complex Liquids. Cambridge University Press, 2003.
[19] R. Metzler and J. Klafter. Phys. Rep., 339:1–77, 2000.
[20] D. ben Avraham and S. Havlin. Diffusion and Reactions in Fractals and Disordered Systems. Cambridge University Press, Cambridge CB2 2RU, UK, 2000.
[21] S. Seeger, K. H. Hoffmann, and C. Essex. J. Phys. A-

Math. Theor., 42:225002, 2009.
[22] O. Mülken and A. Blumen. Phys. Rep., 502:37–87, 2011.
[23] F. Höfling and T. Franosch. Rep. Prog. Phys., 76(4):046602, 2013.
[24] P.-z. Wong and Q.-z. Cao. Phys. Rev. B, 45:7627–7632, 1992.
[25] P. Meakin. J. Sol-Gel Sci. Technol., 15:97–117, 1999.
[26] C. M. Sorensen. Aerosol Sci. Technol., 35:648–687, 2001.
[27] H. Zhao. Chem. Eng. Commun., 192:145–154, 2005.
[28] W. C. K Poon, A. D. Pirie, and P. N. Pusey. Faraday Discuss., 101:65–76, 1995.
[29] T. Onda, S. Shibuichi, N. Satoh, and K. Tsujii. Langmuir, 12:2125–2127, 1996.
[30] M. A Moreles, J. Peña, S. Botello, and R. Iturriaga. Transp. Porous Media, 99:161–174, 2013.
[31] W. Baumgarten and M. J. B. Hauser. EPL, 108:50010, 2014.
[32] D. Stauffer and A. Aharony. Introduction to Percolation Theory. Taylor & Francis Inc., Bristol, PA, revised 2nd edition, 1994.
[33] M. E. J. Newman and R. M. Ziff. Phys. Rev. Lett., 85:4104–4107, 2000.
[34] E. W. Dijkstra. Numerische Mathematik, 1:269–271, 1959.
[35] R. M. Ziff. J. Phys. A-Math. Gen., 32:L457–L459, 1999.
[36] J. Kolafa and M. Rottner. Mol. Phys., 104:3435–3441, 2006.
[37] M. Heinen, E. Allahyarov, and H. Löwen. J. Comput. Chem., 35:275–289, 2014.
[38] J. D. Talman. J. Comput. Phys., 29:35–48, 1978.
[39] P. J. Rossky and H. L. Friedman. J. Chem. Phys., 72:5694–5700, 1980.
[40] A. J. S. Hamilton. Mon. Not. R. Astron. Soc., 312:257, 2000.
[41] V. Krakoviack. Phys. Rev. Lett., 94:065703, 2005.
[42] A. Ikeda and K. Miyazaki. Phys. Rev. Lett., 104:255704, 2010.
[43] P. Charbonneau, A. Ikeda, G. Parisi, and F. Zamponi. Phys. Rev. Lett., 107:185702, 2011.